Check for updates

Adhesion of emulsified oil droplets to hydrophilic and hydrophobic surfaces – effect of surfactant charge, surfactant concentration and ionic strength†

Janneke M. Dickhout,[a] J. Mieke Kleijn,[b] Rob G. H. Lammertink [c] and Wiebe M. de Vos *[c]

Adhesion of emulsified oil droplets to a surface plays an important role in processes such as crossflow membrane filtration, where the oil causes fouling. We present a novel technique, in which we study oil droplets on a model surface in a flow cell under shear force to determine the adhesive force between droplets and surface. We prepared an emulsion of hexadecane and used hydrophilic and hydrophobic glass slides as model surfaces. Different surfactants were used as emulsifiers: negatively charged sodium dodecyl sulphate (SDS), positively charged hexadecyltrimethylammonium bromide (CTAB) and nonionic Triton X-100. We evaluate the role of the surfactant, the glass surface properties and the ionic strength of the emulsion. We found a minimum in the adhesion force between droplets and surface as a function of surfactant concentration. The charged surfactants cause a lower droplet adhesion compared to the nonionic surfactant. The flow cell technique presented here proved to be very useful in understanding the interaction between oil droplets and a surface.

1 Introduction

Oil-in-water emulsions make up many day-to-day products, and are essential for a multitude of industrial processes. However, these emulsions also form some of the largest waste streams from industry. Vegetable oil mills,[1] metal working facilities,[2] fish processing facilities, the leather industry, the dairy industry and the petrochemical industry[3] produce large volumes of oil contaminated water that have to be treated before they can be disposed of. This oily waste water comes into contact with surfaces all through this process, causing problems such as clogging,[4] and fouling in the case of membrane treatment.[5]

The static adhesion of oil droplets, stabilized by a surfactant in water, to a surface has been studied extensively. These fundamental studies mainly concern single droplets with a focus on wetting properties, in order to accurately describe

the forces that play a role in droplet adhesion. Early computational models have described the motion of a solid sphere near a wall with an applied flow.[6,7] Recently Ramon *et al.* developed a model describing the motion and deposition of a rigid particle near a permeable surface, such as a membrane.[8] The model describes the hydrodynamic force on the particle and calculates a possible equilibrium position of the particle in terms of the electrostatic and lubrication forces on the particle. These models can describe the behavior of a particle very close to a surface, but are not able to describe the behavior of a particle or droplet touching the surface. Experimental studies can macroscopically describe the interaction between oil droplets and a surface. Chae Yung *et al.* measured the contact angle of oil droplets on a superoleophobic surface in both an air and water environment.[9] Based upon their measurements of this contact angle for various oleophobic surfaces with different interfacial tensions they proposed a model for the spreading of oil on a surface. Dresselhuis *et al.*[10] studied the spreading of oil droplets stabilized by protein on glass surfaces using microscopy. From the appearance of the droplets at the surface, they could discern between adhered droplets and spread droplets. They found that electrostatic, steric and hydrophobic interactions are the main factors for droplet adhesion and subsequent spreading. Fux and Ramon studied droplet deformation in the presence of permeation through a membrane.[11] They discovered that smaller droplets have a lower deformation propensity compared to bigger oil droplets. When applying crossflow cleaning to remove the oil from the surface, the smaller, spherical droplets could be removed

[a] *Wetsus, European Centre of Excellence for Sustainable Water Technology, Oostergoweg 9, 8911 MA Leeuwarden, The Netherlands*

[b] *Physical Chemistry and Soft Matter, Wageningen University, P.O. Box 8038, 6700EK Wageningen, The Netherlands*

[c] *Membrane Science and Technology, University of Twente, P.O. Box 217, 7500 AE Enschede, The Netherlands. E-mail: w.m.devos@utwente.nl; Tel: +31-534894495*

† Electronic supplementary information (ESI) available: Picture of vapor deposition setup, operation details of flow cell, additional contact angle measurements and images of TX-100 stabilized oil droplets on a hydrophilic and a hydrophobic surface. See DOI: 10.1039/c8sm00476e

whereas the biger, deformed droplets remained attached to the surface.

In contrast to studies that focused on a small number of droplets, work also has been done on emulsions containing large numbers of droplets. The adhesion behavior of emulsified oil droplets is of particular interest in membrane science, where fouling is a major problem.[12] Essafi *et al.* studied the coating of a surface with a monolayer of oil droplets by adding salt to a surfactant stabilized emulsion.[13] By using a flow cell they measured the surface interactions between glass and oil, showing a good agreement between experimental observations and the Langmuir adsorption model, where the adsorption of oil droplets to the surface is treated as a first-order reaction. Malmsten *et al.* studied the formation of a monolayer of droplets on a surface from an emulsion with ellipsometry.[14] In their system, all layers that were formed consisted of droplets with very limited droplet spreading. By considering electrostatic and van der Waals interactions, they could explain the results obtained when varying ionic strength and surfactant type. de Vos *et al.* studied the adhesion of polystyrene particles on a surface covered with polymer brushes under shear force.[15] They used a flow cell, and by applying a shear force they determined the amount of force needed to remove 50% of the adhered particles from the surface. They measured different adhesion strengths for surfaces with different coatings, proving the effectiveness of this setup for studying particle–surface interactions.

In this paper, we aim to combine the fundamentals of surface–droplet interactions with an understanding of what these interactions mean for a large number of droplets as found in emulsions. By studying single droplets and droplets as a population under exactly the same conditions, we can draw a more detailed picture of what happens between droplet and surface. We perform flow cell measurements, in which we let oil droplets adhere to a surface, followed by application of a shear force. Detachment occurs when the shear force becomes larger than the adhesive force. We combine these flow cell measurements with analytical techniques such as reflectometry, contact angle measurements and interfacial tension measurements. By varying the surfactant concentration, surfactant charge and the salt concentration of the emulsion, as well as the hydrophilicity of the surface, we determine the influence of each factor on the adhesion force between the oil droplets and the surface.

2 Materials and methods

2.1 Materials

For preparation of the emulsions and flush solutions, we used DI water, sodium dodecyl sulfate (SDS, Sigma Aldrich 75746), hexadecyltrimethylammonium bromide (CTAB, Sigma Aldrich H6269), Triton X-100 (TX, Sigma Aldrich 9284), *n*-hexadecane (Merck Schuchardt OHG 820633) as the oil and sodium chloride (NaCl, Boom 51275). For glass surface modification we used 1 M sodium hydroxide (NaOH, VWR 31627.290) and trichloro(1*H*,1*H*,2*H*,2*H*-perfluorooctyl)silane (FOTS, Sigma Aldrich 448931). All chemicals were used without further purification steps.

2.2 Emulsion preparation and characterization

To ensure all emulsions have the same characteristics, a stock emulsion was prepared, which was then further diluted to obtain the desired salt and surfactant concentration. The stock emulsions were prepared by dissolving a surfactant (463 mg L^{-1} SDS; 346 mg L^{-1} CTAB; 298 mg L^{-1} TX) in 1 L of DI water in a Duran bottle (Duran 21801545) by mixing with a dispersing mixer (IKA T25 digital Ultra-Turrax with S25N 18G element) for 2 minutes at 14 000 rpm. Then, 2 or 4 g of *n*-hexadecane was injected near the mixer head and mixed for 10 minutes at 14 000 rpm. After resting overnight, the stock emulsion was diluted to contain 1 g L^{-1} hexadecane and the desired surfactant and NaCl concentration. The concentrations of surfactant were chosen to be very close or below the critical micelle concentration (CMC) to avoid formation of micelles. The CMC for SDS is 2400 mg L^{-1}, for CTAB 340 mg L^{-1} and for TX 140 mg L^{-1}. The particle size distribution was determined with a DIPA 2000 – Particle Analyzer (Prolyse). The mean droplet diameter in the diluted emulsions was 3–4 μm and was constant for all conditions.

Surfactant solutions used for rinsing and for applying shear were prepared the same as the emulsions, but without hexadecane and mixing for only 4 minutes. The concentrations of surfactant and NaCl were identical to the emulsion used in each experiment. After preparation, the surfactant solutions were degassed under vacuum and ultrasonic sonication for 15 minutes, followed by 15 minutes of only vacuum. The emulsions were not degassed, as they did not contain as much air bubbles. Furthermore, surfactant solutions were also used for all surfactant adsorption, contact angle and interfacial tension measurements.

2.3 Glass modification and characterization

Glass slides for the flow cell were prepared from microscope glass slides (VWR 631-1552). For the contact angle measurements, the slides were cut to fit the holder for the captive bubble measurement of the contact angle meter before treatment. The silica wafers used for reflectometry (WaferNet S64135) were treated in the same way as the glass after a 70 nm layer of silica oxide was grown on top. This ensures the glass and wafer surfaces are chemically similar. All glass slides were first put in a 1 M NaOH bath for one hour. Afterwards, the glass was flushed with DI water and dried with nitrogen. The dry glass was treated with a Harrick plasma cleaner (Harrick Plasma Cleaner model PDC-002) at the highest setting for one minute. This treatment yielded hydrophilic glass slides with a water contact angle of <5°.

Hydrophobic slides were prepared by vapor deposition of FOTS (a fluorinated trichlorosilane) on hydrophilic glass slides. For this treatment we used a home built vapor deposition setup consisting of three connected glass chambers (Supplementary information 1, ESI†). The first is a gas washing bottle which serves as evaporation chamber. The inlet of the bottle has an injection gate and is connected to a nitrogen flow. The outlet of the evaporation chamber is connected to the reaction chamber where the glass slides are placed. This reaction chamber is connected to a second gas washing bottle filled with water, where the released HCl gas is neutralized. Both evaporation

chamber and reaction chamber can be heated. First, the hydrophilic glass slides were placed in the reaction chamber at 60 °C under a nitrogen flow to dry for at least five hours. After drying, the reaction chamber was left to cool to room temperature. Then, approximately 0.3 mL of FOTS was injected into the evaporation chamber, which was heated to 60 °C. The FOTS was left to evaporate overnight under very low nitrogen flow. In the morning, the nitrogen flow was stopped, the evaporation chamber was left to cool down and the reaction chamber was heated to 60 °C to speed up the reaction of the FOTS with the glass. After one hour, the reaction chamber was left to cool down again, the nitrogen flow was started and about 1 mL of water was injected into the evaporation chamber to neutralize leftover FOTS. After this, the glass slides were removed from the reaction chamber. The contact angle of the hydrophobic glass slides was 108 ± 2°.

2.4 Contact angle and interfacial tension measurements

Both types of measurements were performed on a contact angle and contour analysis instrument (Dataphysics OCA 35). The contact angle measurements were performed in captive bubble mode, where a droplet of hexadecane is captured under a modified glass slide in the aqueous phase. The interfacial tension measurements were performed with the pendant droplet technique, where a droplet of aqueous solution is suspended in hexadecane. Image analysis of the droplet shapes from both contact angle and interfacial tension measurements was performed with the software provided with the measuring instrument, taking into account the density change of the water upon addition of NaCl.

2.5 Reflectometry measurements

The adsorption of surfactant molecules to the surface was measured with reflectometry as described elsewhere.[16] We used solutions with the same concentration of surfactant and NaCl as used for all other experiments. The surfactant molecules were allowed to adsorb to the wafer surface. In between adsorption cycles the cell was flushed with a NaCl solution of the same ionic strength as the surfactant solution. The mass Γ of the surfactant adsorbed to the surface can be calculated as

$$\Gamma = \frac{\Delta S}{S_0} Q \qquad (1)$$

where $\Delta S = S - S_0$, with S the ratio between the p- and s polarized components of the reflected laser beam, S_0 is the starting output signal of the silicon wafer and Q is a sensitivity factor which depends on the angle of incidence of the laser (θ), the refractive indices (n), the thicknesses (d) of the layers of the silicon wafer, and the refractive index increment (dn/dc) of the adsorbate. This factor is 0.100 mg m^{-2} for SDS,[17] 0.151 mg m^{-2} for CTAB[17] and 0.154 mg m^{-2} for TX[18] and a silica layer thickness of 75 nm. The Q-factor thus obtained for these surfactants is 40 mg m^{-2} for SDS, 27 mg m^{-2} for CTAB and 27 mg m^{-2} for TX.

2.6 Flow cell setup

To measure the adhesion of oil droplets in the emulsion to the glass surfaces, a flow cell setup with two parallel plates was used. This flow cell has been used before in the experiments of

Dresselhuis, but in their experiments no shear force was applied.[10] A pulseless pump (Micropump serie 200, Axel Johnson International, Almere, The Netherlands) feeds the emulsion and flow solution into the flow chamber, which was placed under a microscope (Fig. 1). By varying the distance between the plates of the flow cell and the flow of the pump, the hydrodynamic shear-induced force F exerted on the oil droplets in the flow cell is increased and can be calculated as[7,15]

$$F = 10.2\pi R^2 \tau \ (\text{N}) \quad \tau = \frac{6\eta Q}{rh^2} \ (\text{N m}^{-2}) \qquad (2)$$

where R is the droplet diameter, τ is the shear stress at the glass surface, η is the viscosity of the continuous phase, Q is the flow rate of the pump, which varied between 6 and 36 l h^{-1}; r is the channel width and h is the channel height, which varied between 0.7 and 2.3 mm[7] (Supplementary information 2, ESI†). The flow cell was placed under a home built microscope, consisting of a 470 nm LED light source, polkadot beam splitter (Thorlabs BSW10R), 10× objective (Olympus, 10×/0.25), 2× magnification tube lens (Thorlabs ITL200) and a high speed camera (PointGrey GS2-GE-20S4M-C).

2.7 Flow cell operation

Before each experiment, the setup was cleaned by flushing with a 2% ethanol solution at 45 °C for 15 minutes. After this, the system was flushed with DI water at room temperature for 15 minutes. A new modified glass slide was placed in the flow cell and the system was filled with degassed surfactant solution. Then 5 mL of emulsion was injected in the flow cell and left stagnant for 30 minutes to let the droplets float up against the glass. After 30 minutes, the cell was flushed with surfactant solution at the lowest pump setting to remove all oil droplets that did not adhere to the glass surface. After flushing, the channel depth of the flow cell was decreased and the pump speed increased in steps to increase the shear force on the droplets. After each force increment an image of the droplets at the glass surface was captured. All images were taken at the same location in the cell and in the middle of the flow channel to ensure a fully-developed flow.
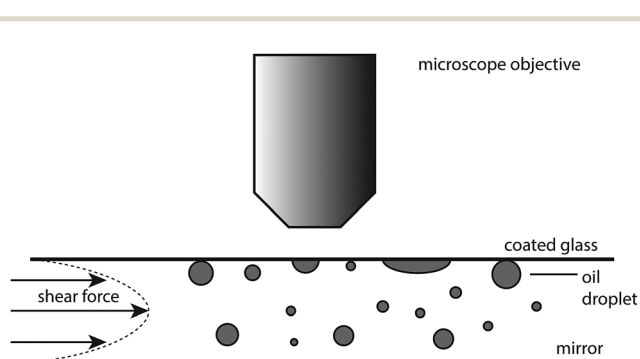

Fig. 1 Schematic representation of the flow cell setup under the microscope. The distance between the mirror and the replaceable upper glass slide can be changed. The shear force is obtained by pumping a solution through the flow cell channel.

2.8 Image analysis

The images taken after each force increment were analyzed with ImageJ to determine the number of droplets adhered to the surface, as well as their mean diameter. Before analysis, the scale of the microscope images was set using a scale grid. First, the background was subtracted (sliding paraboloid, rolling ball radius 50 pixels). Then, the image was sharpened and finally a threshold was applied (default settings). Finally the amount of droplets was counted with a circularity of 0.35–1, which is defined as $4\pi \times$ area/perimeter^2, and a minimum size of 1 μm to exclude dust particles and other artifacts.

After droplet counting, the mean radius was determined from the image taken before flushing. This radius was used to calculate *via* eqn (2) the force on the droplets in all subsequent images. The picture after initial flushing of the cell was considered the starting point of the experiment. The fraction of droplets adhering to the surface are all calculated from the number of droplets in this image.

3 Results and discussion

In this work we have used a range of techniques to study the interaction between oil droplets and a glass surface at different salt and surfactant concentrations, for hydrophilic and hydrophobic surfaces. With reflectometry we measured the adsorption of surfactant molecules from the solution to a silica surface treated similar to the glass surface in the absence of oil. Interfacial tension measurements quantify the amount of surfactant molecules adsorbed to the oil–water interface, without a solid surface present. The contact angle of oil droplets on the surface depends on the hydrophilicity of the surface, which can change in the presence of surfactant molecules. It was measured in a system containing all the components present in the flow cell system, but in the absence of shear force. With these background measurements, we then moved on to our flow cell approach. Our subsequent observations on droplet adhesion in the flow cell provide a measure of the strength of droplet–surface interactions, and also allow direct visual observation.

3.1 Surfactant adsorption

[h] reflectometry is widely used to study the adsorption of molecules to surfaces.[19–22] In this section, we discuss the adsorption of SDS, CTAB and TX to a hydrophilic, negatively charged silica surface and to an uncharged hydrophobic surface. As expected, SDS, which is negatively charged, shows low adsorption to the hydrophilic, negatively charged surface (Fig. 2a and b).[23] The little adsorption that is measured is probably due to impurities in the solution. SDS is sensitive to hydrolysis of the head group from the dodecane tail, leading to minute amounts of dodecanol in the solution, especially below the CMC.[24] The hydrophobic tails of SDS molecules do adsorb to the hydrophobic surface to form a monolayer. Therefore, the hydrophobic surface becomes negatively charged in the presence of SDS.[25]

Firstly, we measured the SDS adsorption at three different surfactant concentrations: 115 mg L^{-1}, 231 mg L^{-1} and 463 mg L^{-1} (Fig. 2a) with 10 mM NaCl added. No significant difference in the amount of surfactant adsorbed to the hydrophobic surface was observed, indicating that the surface is saturated with surfactant molecules, giving it a constant negative charge.

Secondly, we varied the salt concentration of the solution with 231 mg L^{-1} SDS, adding 1, 10 and 100 mM NaCl. There seems to be a maximum in the adsorbed amount of surfactant at 10 mM NaCl for both hydrophilic and hydrophobic surfaces (Fig. 2b). It has been observed that the amount of surfactant adsorbed to a surface increases until concentrations close to the CMC of the surfactant. At higher concentrations the amount of adsorbed surfactant decreases again.[25] This effect is attributed to impurities in the used surfactant. Dodecanol is expected to adsorb stronger to the silica–water interface than SDS, forming dense monolayers.[26] The increased salt concentration possibly influences this adsorption, for instance by influencing the adsorption strength of dodecanol to the interface. The exact mechanism however is not clear. Generally speaking, it can be stated that at different salt concentrations both the hydrophilic and the hydrophobic surfaces are negatively charged, the latter due to SDS adsorption.

Finally we compared the adsorption of anionic SDS to cationic CTAB and nonionic TX to study the influence of surfactant head group charge (Fig. 2c). CTAB, which is positively charged, forms a double layer on the hydrophilic, negatively charged surface, resulting in a positively charged surface.[27] On the hydrophobic surface, CTAB forms a monolayer, also resulting in a positively charged surface. This means that for charged surfactants, the hydrophobic surface will possess the same
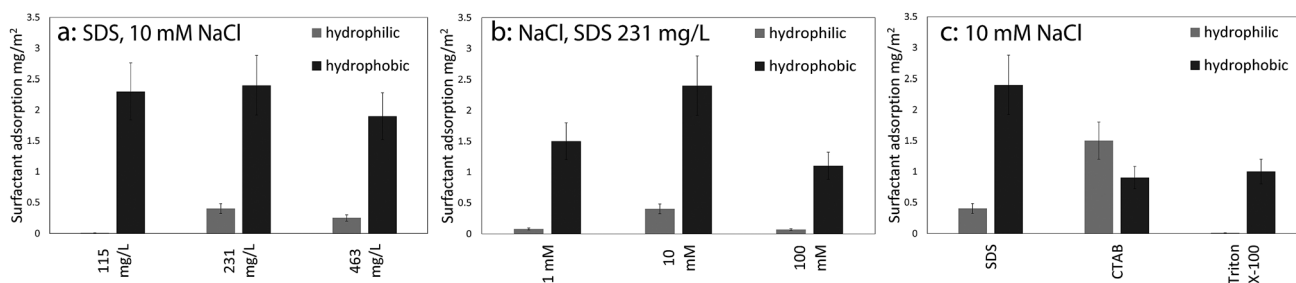

Fig. 2 Surfactant adsorption to hydrophilic and hydrophobic surfaces for (a) different SDS concentrations and 10 mM NaCl; (b) different NaCl concentrations and 231 mg L^{-1} SDS; (c) surfactants with different properties at 10 mM NaCl and 231 mg L^{-1} SDS, 176 mg L^{-1} CTAB and 149 mg L^{-1} TX. Error bars are 15% of the measured mean after three repetitions.

charge as the surfactant present. The nonionic surfactant TX however, does not adsorb to the hydrophilic surface, but does adsorb to the hydrophobic surface. The hydrophobic surface becomes more hydrophilic because of the polar headgroups pointing outwards into the aqueous phase.[28] The hydrophilic head group of TX consists of a short polyethylene oxide (PEO) tail. The adsorption of PEO to silica is strongly dependent on pH[29,30] and decreases upon the addition of salt.[31] At increasing pH the adsorption of PEO on silica decreases, especially above pH 8.

3.2 Interfacial tension surfactant solution/oil

The interfacial tension between the surfactant solution and oil, which correlates to the adsorption of surfactant in the oil–water interface, was measured using the pendant droplet technique, in which a droplet of surfactant solution was suspended in hexadecane. From the interfacial tension it is possible to estimate the amount of surfactant adsorbed to the oil interface using the generalized form of the Gibbs adsorption isotherm

$$-\mathrm{d}\gamma = RT \sum \Gamma_i \mathrm{d} \ln a_i \tag{3}$$

where γ represents the interfacial tension, and Γ_i and a_i the surface excess and the activity of the ith ionic species in solution respectively.[32]

With increasing surfactant concentration, the interfacial tension (at 10 mM NaCl) lowers from 22 mN m^{-1} for 115 mg L^{-1} SDS and 18 mN m^{-1} for 231 mg L^{-1} SDS to 14 mN m^{-1} for 463 mg L^{-1} SDS (Fig. 3I, III and V). The amount of surfactant adsorbed to the interface was estimated to be 1.6 µmol m^{-2}, 3.1 µmol m^{-2} and 4.0 µmol m^{-2} respectively. This behavior indicates that the interface between oil and water is not saturated and more surfactant molecules adsorb at increasing surfactant concentration. This is expected as the used surfactant concentrations are below the CMC.[33]

At increasing NaCl concentration in the presence of 231 mg L^{-1} SDS, the interfacial tension lowers (Fig. 3II, III and IV). The positively charged sodium ions screen the charge of the negatively charged SDS head groups. This lowers the electrostatic repulsion between the head groups, allowing more surfactant molecules to adsorb, thus lowering the interfacial tension from 22 mN m^{-1} for 1 mM NaCl and 18 mN m^{-1} for 10 mM NaCl to 7 mN m^{-1} for 100 mM NaCl. From these values, we estimated the amount of surfactant on the interface to be 2.5 µmol m^{-2}, 3.1 µmol m^{-2} and 3.3 µmol m^{-2} respectively. In addition to this, the colloidal stability of the emulsion might go down as the electrostatic repulsion between the droplets is also screened by the sodium ions. When comparing SDS at 231 mg L^{-1}, CTAB at 176 mg L^{-1} and TX at 149 mg L^{-1}, all in the presence of 10 mM NaCl, it is evident that CTAB results in the lowest interfacial tension at 1 mN m^{-1}, followed by TX (13 mN m^{-1}) and SDS (18 mN m^{-1}).

3.3 Contact angle measurements

The contact angle between an oil droplet and the glass surface immersed in surfactant solution was measured with the captive droplet technique, where the oil droplet is trapped under the glass.
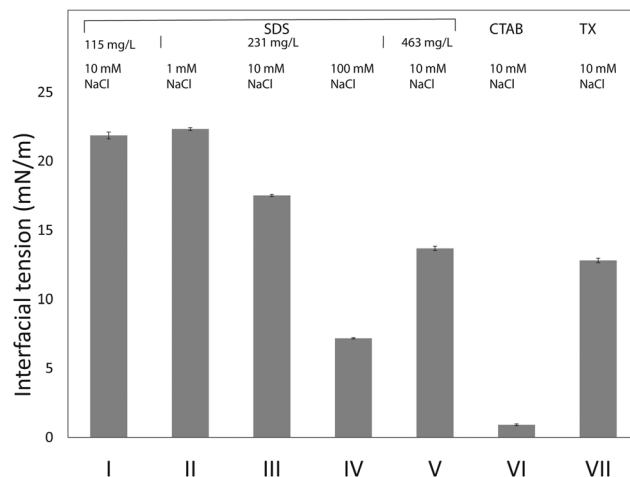

Fig. 3 Interfacial tension of the oil–water interface in presence of surfactant. (I) 115 mg L^{-1} SDS 10 mM NaCl; (II) 231 mg L^{-1} SDS, 1 mM NaCl; (III) 231 mg L^{-1} SDS, 10 mM NaCl; (IV) 231 mg L^{-1} SDS, 100 mM NaCl (V) 463 mg L^{-1} SDS, 10 mM NaCl; (VI) 176 mg L^{-1} CTAB, 10 mM NaCl; (VII) 149 mg L^{-1} TX, 10 mM NaCl. Error bars represent the standard deviation after duplicates.

On a hydrophilic surface, the oil droplet has a contact angle of about 150° for all surfactant and NaCl concentrations (Fig. 4). In the case of SDS the surface of the oil droplet is covered by negatively charged surfactant molecules, whereas the surface is negatively charged by itself causing electrostatic repulsion and avoiding contact. The droplet retains its spherical shape and rolls over the surface, indicating no real attachment. Because the oil droplets roll away, the contact angle was measured directly after touching the surface. For hydrophobic surfaces however, the droplet collapses into a hemispherical shape with a contact angle of about 60° upon contact with the surface.
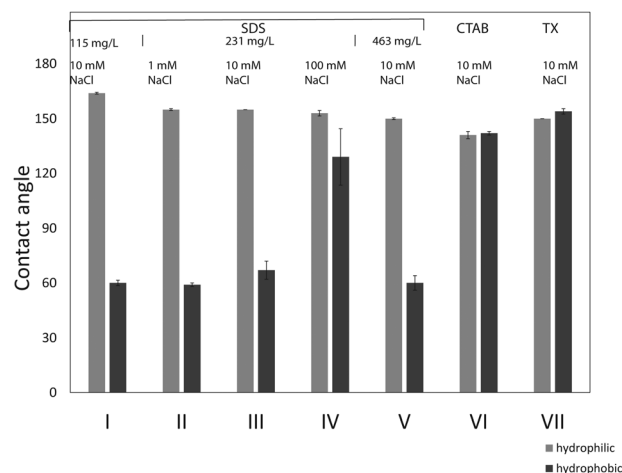

Fig. 4 Contact angles of surfactant stabilized hexadecane droplets on glass measured with the captive bubble method. Contact angle was measured through the droplet upon contact with the surface. (I) 115 mg L^{-1} SDS 10 mM NaCl; (II) 231 mg L^{-1} SDS, 1 mM NaCl; (III) 231 mg L^{-1} SDS, 10 mM NaCl; (IV) 231 mg L^{-1} SDS, 100 mM NaCl (V) 463 mg L^{-1} SDS, 10 mM NaCl; (VI) 176 mg L^{-1} CTAB, 10 mM NaCl; (VII) 149 mg L^{-1} TX, 10 mM NaCl. Error bars represent the standard deviation after duplicates.

The contact angles after 30 minutes can be found in Supplementary information 3 (ESI†). In these circumstances, the repulsive force between the glass surface covered by a monolayer of SDS molecules and the droplet covered in SDS molecules is overcome by the hydrophobic interactions between the surface and the oil. An exception we observed was the measured contact angle at an SDS concentration of 231 mg L^{-1}, 100 mM NaCl and the hydrophobic surface (Fig. 4IV). In this experiment, we observed that the oil droplet retained its spherical shape upon contact with the surface. After 2–3 seconds the droplet collapsed, like observed in all other experiments with SDS on the hydrophobic surface. This indicates that at sufficiently high surfactant adsorption to both surface and oil–water interface, a barrier is formed that can avoid immediate droplet collapse.

When comparing SDS with CTAB and TX at 10 mM NaCl, it becomes immediately clear that droplets stabilized by CTAB and TX do not collapse on a hydrophilic surface and retain their spherical shape. In the case of CTAB, the repulsive electrostatic force between droplet and the glass surface covered in either a mono- or bilayer of surfactant is sufficient to keep the droplet from collapsing on the surface. For TX, which is a surfactant without charge, the repulsion is caused by only sterical hindrance between the surface and the oil droplet.

3.4 Flow cell

The flow cell is used to visually observe droplet adhesion to the surface. In contrast to the contact angle measurements in Fig. 4, the droplets are seen from above rather than from the side. The oil droplets studied in the flow cell are much smaller, leading to less deformable droplets. The components present in both contact angle measurements and flow cell experiments are the same.

When the emulsion is injected in the cell, due to buoyancy the droplets float up and attach to the top glass plate of the cell (Fig. 1). With a light microscope, we can observe the droplets on this glass surface (Fig. 5). After 30 minutes without any flow, the surface is covered in oil droplets (Fig. 5, first column). We then remove the droplets that are not attached to the surface by gently flushing the flow cell with surfactant solution until only the droplets remain that have truly attached to the surface (Fig. 5, second column).

In contrast to the contact angle measurements from Section 3.3, adhesion of droplets is observed on both the hydrophilic and the hydrophobic surface, which we attribute to a longer contact time. The state after flushing is the starting point of the experiment. Then, by increasing the shear force on the droplets, we wash away a fraction of the attached droplets, until we reach maximum pump capacity and minimum plate distance (Fig. 5, third and fourth column). In our experiments, we did not observe coalescence of droplets on the surface. In addition, due to sufficiently high shear force, removed droplets were immediately flushed away. We also observed that on the hydrophobic surface, a small number of oil droplets stabilized by SDS or CTAB spread out on the surface. After this happens, it is impossible to wash the oil from the surface. We did not observe this behavior on the hydrophilic surface for the charged surfactants, but oil droplets stabilized by TX spread out on both hydrophilic and hydrophobic surfaces. This indicates that electrostatic repulsion plays an important role in the force balance of the interaction between surface and oil droplet.

3.4.1 Surfactant concentration. The fraction of droplets adhering to the hydrophilic and hydrophobic glass surface at different SDS concentrations and 10 mM NaCl is plotted in Fig. 6. At higher applied shear forces, droplets detach from the surface. We performed the experiment for three different SDS concentrations with 10 mM NaCl. On the hydrophilic surface,
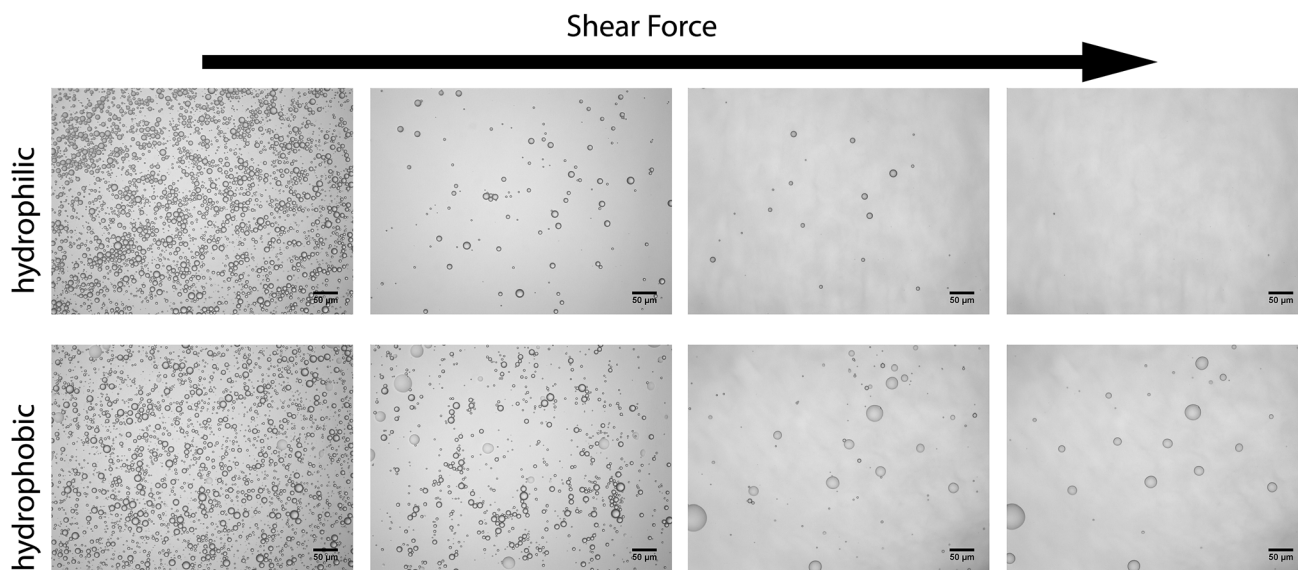

Fig. 5 Photos from the flow cell setup showing droplets stabilized by SDS (231 mg L^{-1}) on a hydrophilic and hydrophobic surface under increasing shear force. The pictures are taken after the stagnant phase, flushing, in the middle of the experiment and after the experiment. Note the spreading of droplets on the hydrophobic surface.
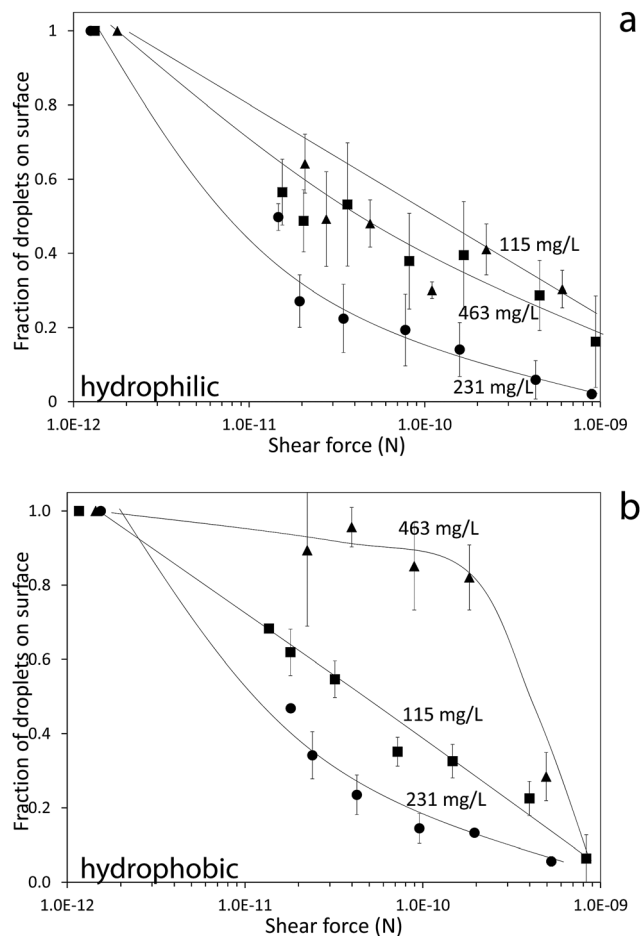
Fig. 6 Fraction of droplets that sticks to a hydrophilic (a) and hydrophobic (b) surface for different SDS concentrations and a NaCl concentration of 10 mM. Error bars represent standard deviation after duplicates. Lines are a guide to the eye.

we observed comparable detachment behavior for 115 mg L^{-1} and 463 mg L^{-1} of SDS. At 231 mg L^{-1} SDS, the detachment of droplets from the surface is much faster. On the hydrophobic surface, we observed the fastest droplet detachment for 231 mg L^{-1} SDS, a slightly slower detachment for 115 mg L^{-1} SDS and the least droplet detachment for 463 mg L^{-1} SDS. This indicates that the droplet adhesion at 231 mg L^{-1} SDS is the weakest, both on the hydrophilic and the hydrophobic surface, and we observe a minimum in the adhesive force between droplet and surface at this surfactant concentration. As shown before in Fig. 2, SDS adsorbs to the hydrophobic surface, providing the surface with a negative charge, and the hydrophilic surface is negatively charged due to dissociation of silanol groups. In addition, a small amount of surfactant also adsorbs on the hydrophilic surface at 231 mg L^{-1} SDS. The droplet surface is also covered by SDS molecules, so electrostatic repulsion prevents droplets from adhering. The minimum in droplet–surface interaction can be explained by a balance of various processes taking place at the surface. At increasing surfactant concentration, the interfacial tension of the oil droplet decreases, as discussed in Section 3.2. This means more

surfactant molecules are adsorbed to the oil–water interface and a higher surface charge density, increasing the electrostatic repulsion between droplet and surface. In contrast to what we expected, a higher amount of surfactant did not yield a lower adhesion force to the surface, so other factors play a role in this adhesion behavior. The deformability of oil droplets can be described by the capillary number Ca = $\tau R/\gamma$.[34] As shown by Gupta and Basu, deformation of oil droplets occurs at capillary numbers in the order of 1×10^{-2} and higher.[35] The capillary number of our droplets is lower, in the order of 1×10^{-3} indicating that droplet deformation does not play a role in the adhesion behavior of our system. Finally, the viscosity of the aqueous phase does not change significantly at our concentrations of surfactant, so the effects of shear thinning can be omitted.[36] However, we did observe that at 231 mg L^{-1} SDS there is a maximum in surfactant adsorption to both the hydrophilic and the hydrophobic surface, which can explain the decreased interaction between surface and droplets. Thus, it remains unclear why the droplet adhesion increases with increasing SDS concentration.

3.4.2 NaCl concentration. As shown in Section 3.1, both the hydrophilic and hydrophobic surface are negatively charged at all NaCl concentrations, because of the properties of the silica itself and the adsorption of SDS respectively (Fig. 2a). At increasing NaCl concentration, the surface tension decreases, because more surfactant molecules adsorb to the oil–water interface, thus increasing the charge density of the droplet surface, as discussed in Section 3.2.

For both surfaces, droplet adhesion at 1 and 10 mM is comparable. At 100 mM, however, the adhesion of droplets to the surfaces increases. More shear force is required to wash away the oil droplets. At high salt concentrations, the counter-ions (in this case sodium) allow for more SDS adsorption on the oil–water interface, but also screen the resulting surface charge of the droplet and the glass surface. The repulsive force between droplet and surface decreases and droplets can adhere to the surface more strongly. Calculating the electrostatic repulsion of the system with the DLVO equation indicates that the van der Waals and electrostatic forces are in the same order of magnitude as the shear force applied to the droplets, which indicates that electrostatic interactions play a significant role in the droplet adhesion. The force at which droplets detach from the surface is about 2×10^{-10} N for the hydrophilic surface, and 3×10^{-11} N for the hydrophobic surface. This means the interaction between the droplets and the surface is stronger for the hydrophilic surface. This suggests that the presence of a surfactant layer on the surface, as in the hydrophobic case, is better at preventing droplets to adhere to the surface at this salt concentration. As shown by Tadros and Lyklema, the surface charge of glass at neutral pH and 10 mM NaCl is -0.05 C m^{-2},[37] whereas the adsorption of surfactant yields a surface charge of -0.8 C m^{-2}. In addition two layers of surfactant (one of the droplet and one on the surface) form a better barrier than just one layer of surfactant. We did observe, however, that a small fraction of droplets spreads out on the hydrophobic surface. These droplets make contact with the surface and collapse to
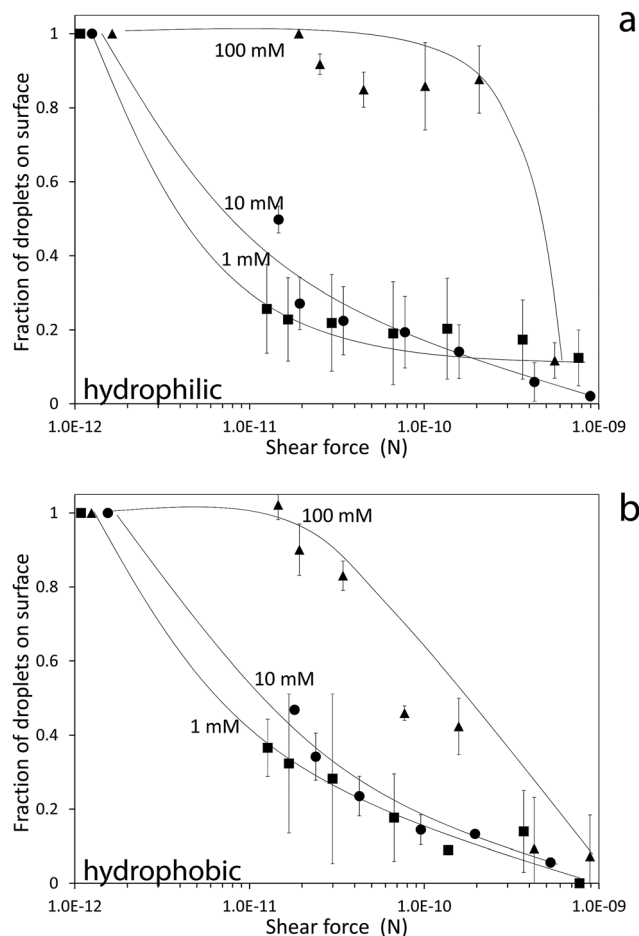
Fig. 7 Fraction of droplets that sticks to a hydrophilic (a) and hydrophobic (b) surface for different NaCl concentrations and an SDS concentration of 231 mg L^{-1}. Error bars represent standard deviation after duplicates. Lines are a guide to the eye.
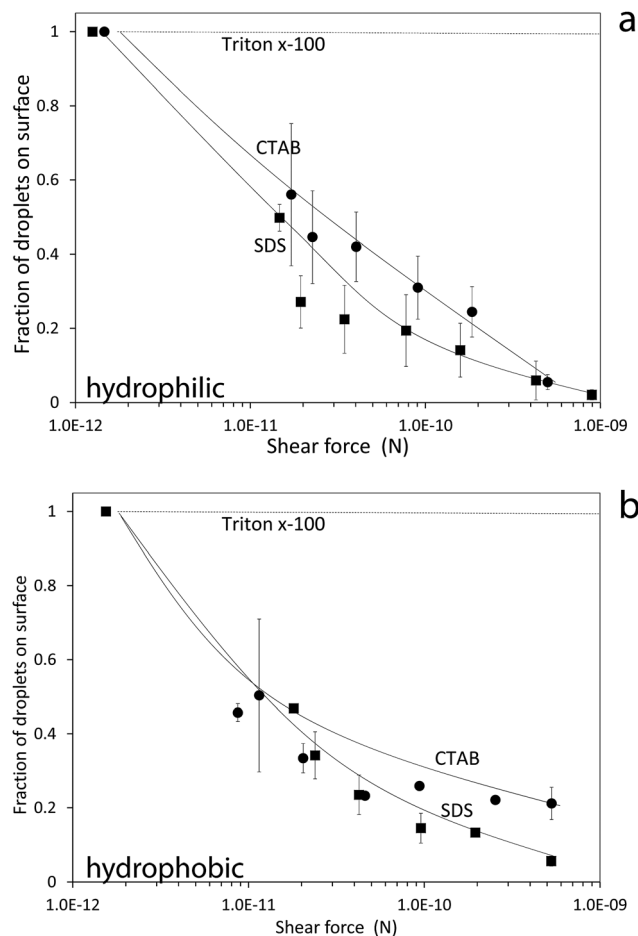

Fig. 8 Fraction of droplets that sticks to a hydrophilic (a) and hydrophobic (b) surface for different surfactants and 10 mM NaCl. Error bars represent standard deviation after duplicates. Lines are a guide to the eye.

form spread out patches of oil, see also Fig. 5. These patches of oil cannot be removed from the surface by washing with surfactant solution. This behavior was not observed on the hydrophilic surface for SDS (Fig. 7).

3.4.3 Surfactant type. The charge of the surfactant used to stabilize the emulsion influences the behavior of oil droplets on the surface. We compared three surfactants, anionic SDS, cationic CTAB and nonionic TX (Fig. 8). For both the hydrophilic and hydrophobic surface similar trends were observed. Both SDS and CTAB result in equal sign charge for surface and droplet, allowing for droplets to be washed away. TX however behaves differently. Oil droplets adhere to the surface in aggregates and have a high tendency to spread on both the hydrophilic and the hydrophobic surface (Supplementary information 4, ESI†). Images taken in the experiments with TX were not suitable for image analysis because of very high droplet coverage, therefore the line in the graph is based on this general observation rather than data from the images. The lack of ionic repulsion between the interface and the oil droplets allows for higher adhesion, and much easier spreading.

4 Conclusion

In this article we used a novel flow cell technique to study the adhesion strength between a glass surface by applying a shear force. Because the flow cell allowed us to visually observe the droplets, we could also see the behavior of the individual oil droplets on the surface. By using hydrophilic and hydrophobic surface modifications, the role of the surface in droplet adhesion could be studied. In addition to these flow cell measurements, we performed interfacial tension, surfactant adsorption and contact angle measurements under similar conditions. With these techniques, we were able to study the influence of surfactant concentration, NaCl concentration and surfactant charge on the adhesion behavior of droplets to hydrophilic and hydrophobic surfaces.

Firstly, there appears to be an ideal surfactant concentration for SDS to prevent droplet adhesion to both hydrophilic and hydrophobic surfaces. Secondly, at increasing salt concentrations, droplets adhere to both the hydrophilic and the hydrophobic surface. At 100 mM NaCl, droplets adhere even stronger to the hydrophilic than to the hydrophobic surface. In addition, droplets also tend to spread out on the hydrophobic surface. Finally, we

compared two charged surfactants, SDS and CTAB, to an uncharged surfactant. TX. Where the charged surfactants showed similar behavior, where droplets could be washed away from the surface, the droplets stabilized with uncharged surfactant either aggregated or spreaded on both the hydrophilic and the hydrophobic surface. The results presented in this paper show that the flow cell gives us an adequate technique to study the interaction of oil droplets and surfaces, and should be used to study more complex droplet–surface systems.

Conflicts of interest

There are no conflicts to declare.

Acknowledgements

References

1 X. Zhu, W. Tu, K.-H. Wee and R. Bai, *J. Membr. Sci.*, 2014, **466**, 36–44.

2 A. Murić, I. Petrinić and M. L. Christensen, *Chem. Eng. J.*, 2014, **255**, 403–410.

3 J. Zheng, B. Chen, W. Thanyamanta, K. Hawboldt, B. Zhang and B. Liu, *MPB*, 2016, **104**, 7–19.

4 T. Wallace, D. Gibbons, M. O'Dwyer and T. P. Curran, *J. Environ. Manage.*, 2017, **187**, 424–435.

5 S. Alzahrani and A. W. Mohammad, *J. Water Process Eng.*, 2014, **4**, 107–133.

6 A. Goldman, R. Cox and H. Brenner, *Chem. Eng. Sci.*, 1967, **22**, 637–651.

7 A. Goldman, R. Cox and H. Brenner, *Chem. Eng. Sci.*, 1967, **22**, 653–660.

8 G. Z. Ramon, H. E. Huppert, J. R. Lister and H. A. Stone, *Phys. Fluids*, 2013, **25**, 073103.

9 Y. Chae Jung and B. Bhushan, *Langmuir*, 2009, **25**, 14165–14173.

10 D. M. Dresselhuis, G. A. van Aken, E. H. A. de Hoog and M. A. Cohen Stuart, *Soft Matter*, 2008, **4**, 1079–1085.

11 G. Fux and G. Z. Ramon, *Environ. Sci. Technol.*, 2017, **51**, 13842–13849.

12 J. Dickhout, J. Moreno, P. Biesheuvel, L. Boels, R. Lammertink and W. de Vos, *J. Colloid Interface Sci.*, 2017, **487**, 523–534.

13 W. Essafi, K. Wong, J. Bibette and P. Poulin, *J. Colloid Interface Sci.*, 2005, **286**, 730–738.

14 M. Malmsten, A.-L. Lindström and T. Wärnheim, *J. Colloid Interface Sci.*, 1996, **179**, 537–543.

15 W. M. de Vos, A. de Keizer, M. A. Cohen Stuart and J. M. Kleijn, *Colloids Surf., A*, 2010, **358**, 6–12.

16 J. de Grooth, M. Dong, W. M. de Vos and K. Nijmeijer, *Langmuir*, 2014, **30**, 5152–5161.

17 T. Tumolo, L. Angnes and M. S. Baptista, *Anal. Biochem.*, 2004, **333**, 273–279.

18 G. Csucs and J. J. Ramsden, *Biochim. Biophys. Acta*, 1998, **1369**, 304–308.

19 J. Dijt, M. A. Cohen Stuart, J. Hofman and G. Fleer, *Colloids Surf.*, 1990, **51**, 141–158.

20 J. Dijt, M. A. Cohen Stuart and G. Fleer, *Adv. Colloid Interface Sci.*, 1994, **50**, 79–101.

21 W. M. de Vos, P. M. Biesheuvel, A. de Keizer, J. M. Kleijn and M. A. Cohen Stuart, *Langmuir*, 2008, **24**, 6575–6584.

22 M. Jiang, I. Popa, P. Maroni and M. Borkovec, *Colloids Surf., A*, 2010, **360**, 20–25.

23 M. Ishiguro and L. K. Koopal, *Adv. Colloid Interface Sci.*, 2016, **231**, 59–102.

24 D. A. Woods, J. Petkov and C. D. Bain, *J. Phys. Chem. B*, 2011, **115**, 7353–7363.

25 K. Hu and A. J. Bard, *Langmuir*, 1997, **13**, 5418–5425.

26 R. N. Ward, D. C. Duffy, P. B. Davies and C. D. Bain, *J. Phys. Chem.*, 1994, **98**, 8536–8542.

27 E. Tyrode, M. W. Rutland and C. D. Bain, *J. Am. Chem. Soc.*, 2008, **130**, 17434–17445.

28 H. Tang, L. Zhao, W. Sun, Y. Hu and H. Han, *Colloids Surf., A*, 2016, **509**, 323–333.

29 J. Rubio and J. Kitchener, *J. Colloid Interface Sci.*, 1976, **57**, 132–142.

30 G. Van der Beek and M. A. Cohen Stuart, *J. Phys.*, 1988, **49**, 1449–1454.

31 D. Nevskaia, A. Guerrero-Ruíz and J. de D. López-González, *J. Colloid Interface Sci.*, 1998, **205**, 97–105.

32 K. Tajima, *Bull. Chem. Soc. Jpn.*, 1971, **44**, 1767–1771.

33 T. D. Gurkov, D. T. Dimitrova, K. G. Marinova, C. Bilke-Crause, C. Gerber and I. B. Ivanov, *Colloids Surf., A*, 2005, **261**, 29–38.

34 N. Müller-Fischer, P. Tobler, M. Dressler, P. Fischer and E. J. Windhab, *Exp. Fluids*, 2008, **45**, 917–926.

35 A. K. Gupta and S. Basu, *Chem. Eng. Sci.*, 2008, **63**, 5496–5502.

36 A. M. Poskanzer and F. C. Goodrich, *J. Phys. Chem.*, 1975, **79**, 2122–2126.

37 T. Tadros and J. Lyklema, *J. Electroanal. Chem. Interfacial Electrochem.*, 1968, **17**, 267–275.